Published online December 2, 2004

Nucleic Acids Research, 2004, Vol. 32, No. 21 ***e169***
doi:10.1093/nar/gnh167

In vitro selection of Jun-associated proteins using mRNA display

Kenichi Horisawa, Seiji Tateyama, Masamichi Ishizaka, Nobutaka Matsumura, Hideaki Takashima, Etsuko Miyamoto-Sato, Nobuhide Doi and Hiroshi Yanagawa*

Department of Biosciences and Informatics, Faculty of Science and Technology, Keio University, Yokohama 223-8522, Japan

Received October 5, 2004; Revised and Accepted November 11, 2004

ABSTRACT

Although yeast two-hybrid assay and biochemical methods combined with mass spectrometry have been successfully employed for the analyses of protein–protein interactions in the field of proteomics, these methods encounter various difficulties arising from the usage of living cells, including inability to analyze toxic proteins and restriction of testable interaction conditions. Totally *in vitro* display technologies such as ribosome display and mRNA display are expected to circumvent these difficulties. In this study, we applied an mRNA display technique to screening for interactions of a basic leucine zipper domain of Jun protein in a mouse brain cDNA library. By performing iterative affinity selection and sequence analyses, we selected 16 novel Jun-associated protein candidates in addition to four known interactors. By means of real-time PCR and pull-down assay, 10 of the 16 newly discovered candidates were confirmed to be direct interactors with Jun *in vitro*. Furthermore, interaction of 6 of the 10 proteins with Jun was observed in cultured cells by means of co-immunoprecipitation and observation of subcellular localization. These results demonstrate that this *in vitro* display technology is effective for the discovery of novel protein–protein interactions and can contribute to the comprehensive mapping of protein–protein interactions.

INTRODUCTION

Comprehensive analysis of protein–protein interactions is an important task in the field of proteomics, functional genomics and systems biology. Protein–protein interactions are usually analyzed by means of biochemical methods such as pull-down assay and co-immunoprecipitation, yeast two-hybrid (Y2H) assay and phage display. Recently, the combined use of mass spectrometry (MS) with an affinity tag (1) has made the biochemical methods more comprehensive and reliable. However, the testable interaction conditions are restricted by the properties of the biological sources. The Y2H assay is one of the major tools used in the discovery and characterization of protein–protein interactions (2). However, the results of Y2H analyses often include many false positives due to auto-activating bait or prey fusion proteins (3) and interactions of proteins that are toxic to yeast cells cannot be examined. Phage display, the most widely used display technology (4), is an effective alternative, because the interactions between libraries and target proteins occur *in vitro*, allowing optimal conditions to be used for many different target proteins. Further, very low copy number proteins can be identified by repeating the selection round. However, the use of phage display is similarly limited, because phage libraries are produced in living bacteria (5).

Totally *in vitro* display technologies such as ribosome display (6,7), mRNA display (8–10) and DNA display (11) can circumvent the above difficulties, because they do not need living cells. In mRNA display, a library of genotype–phenotype linking molecules is constructed in which mRNA (genotype) binds to protein (phenotype) through puromycin during cell-free translation. After affinity selection via the protein moiety of the molecules in the library, the mRNA moiety of the selected molecules can be amplified by means of RT–PCR. By performing iterative selection, very low copy number proteins can be detected from large-scale cDNA libraries, routinely in the range of 10^{13} members. In 1997, the prototype of mRNA display was originally developed in our laboratory and that of Szostak independently, and the conjugate of protein with its encoding mRNA was named *in vitro* virus (IVV) (8,9) and RNA–peptide fusion (10), respectively. So far, RNA–peptide fusion has been applied to the selection of various functional peptides and antibody mimics (12,13), but the application to protein–protein interaction analysis has been limited (14,15). Recently, we improved the stability of the template mRNA for IVV molecules and the efficiency of IVV formation by employing a polyethylene glycol (PEG) spacer and wheat germ cell-free translation system (16) to improve the selection ability of the IVV technique. In this study, we applied the improved IVV technique to the screening of protein–protein interactions. As a model bait protein, we chose a basic leucine zipper (bZIP) domain of Jun protein, an important transcription factor, to screen Jun interactors from a mouse brain cDNA library. The screening afforded several known and unknown Jun-associated protein candidates, and we confirmed that many

*To whom correspondence should be addressed. Tel: +81 45 566 1775; Fax: +81 45 566 1440; Email: hyana@bio.keio.ac.jp

of the candidates interacted directly with Jun, not only *in vitro*, but also in cultured cells, by using pull-down assay and co-immunoprecipitation assay. These results demonstrate that our *in vitro* display technology is effective for discovery of novel protein–protein interactions and can contribute to the comprehensive mapping of protein–protein interactions.

METHODS

Preparation of bait template RNA

The cDNA of mouse Jun (167–319 amino acids) was amplified by PCR using a forward primer (5′-CCGCGGGATCCCCG-GTCTACGCCAACCTC-3′) containing a BamHI site and a reverse primer (5′-CACCCCTCGAGAACGTGGTTCATGA-CTTTCTGCTTA-3′) containing an XhoI site, and digested with BamHI and XhoI. The fragment was subcloned into the BamHI/XhoI site of pCMV-CBPzz vector (16), which contains a SP6 promoter, a part of the omega sequence named O′ (5′-ACAATTACTATTTACAATTACA-3′) (17), an N-terminal T7-tag coding sequence, and a C-terminal TAP tag coding sequence (1). From the resulting plasmid pCMV-JunCBPzz, a bait template DNA was PCR-amplified with primers 5′SP6(0′)T7 (5′- GAATTTAGGTGACACTAT-AGAAACAATTACTATTTACAATTACAATGGCTAGCA-TGACTGGTGGACAG-3′) and 3′FosCBPzz (5′-GGATCTC-CATTCGCCATTCA-3′). The PCR product was purified with a QIAquick PCR purification kit (Qiagen). The purified DNA was used as a template for *in vitro* transcription with a RiboMax large-scale RNA production system-SP6 (Promega). The RNA was purified with an RNeasy mini kit (Qiagen).

Preparation of IVV template RNA library

The architecture of IVV was described previously (16). Mouse brain poly(A)$^+$ RNA (BD Biosciences) was primed using the oligonucleotide 5′-TCGTCATCGTCCTTGTA-GTCAAGCTTN$_9$-3′ and cDNA was synthesized using a SuperScript double strand cDNA synthesis kit (Invitrogen). The cDNA was ligated with adaptor DNA (forward oligonucleotide: 5′-TAGCATGACTGGTGGACAGCAAATGGGT-GCGGCCGCGAATTCC-3′; reverse oligonucleotide: 5′-GGA-ATTCG-3′) using a Ligation High kit (Toyobo). After ethanol precipitation, the ligated DNA was PCR-amplified with primers, 5′F3 (5′-GGAAGATCTATTTAGGTGACACTATAGAACAA-CAACAACAACAAACAACAACAAAATG-3′) and 3′lib_PCR (5′-TTTTTTTTCTTGTCGTCATCGTCCTTGTAGTC-3′). The PCR product was purified with the QIAquick PCR purification kit and fractionated (over ~200 bp) with a CHROMA SPIN-1000 (BD Biosciences). The fractionated PCR product was used as a template for transcription using the RiboMax large RNA production system-SP6. The resulting RNA was ligated with PEG Puro spacer [p(dCp)2-T(Fluor)p-PEGp-(dCp)2-puromycin] using T4 RNA ligase (Takara). The ligated RNA was purified with the RNeasy mini kit.

Affinity screening

The IVV formation reaction was performed as described previously (16), with some modifications. Briefly, a 50 µl aliquot of wheat germ extract reaction mixture (Promega) containing 10 pmol of the bait Jun RNA, 10 pmol of the ligated library RNA, 80 µM amino acid mixture, 76 mM potassium acetate and 40 U of RNase inhibitor (Invitrogen) was incubated for 1 h at 26°C. Subsequently, the reaction mixture was added to 50 µl of rabbit immunoglobulin G (IgG) agarose beads (Sigma) equilibrated with 50 µl of IPP150 buffer (10 mM Tris–HCl, pH 8.0, 150 mM NaCl and 0.1% NP-40), and mixed on a rotator for 2 h at 4°C. The beads were washed with 800 µl of IPP150 buffer once and with 800 µl of TEV cleavage buffer (10 mM Tris–HCl, pH 8.0, 150 mM NaCl, 0.1% NP-40, 0.5 mM EDTA and 1 mM DTT) five times, then 100 µl of TEV cleavage buffer containing 100 U of TEV protease was added, and rotation was continued for 2 h at 16°C. The resulting eluate was used as the RT–PCR template. RT–PCR was performed with a OneStep RT–PCR kit (Qiagen) using primers, 5′F3 and 3′Flag-1AL (5′-TTTTTTTTCTTGTCGTCATCG-TCCTTGTAG-3′). The optimal number of PCR cycles without reaching a plateau was 26–30 cycles at each RT–PCR step. The RT–PCR product was used for the next round of selection as described above. After five rounds of affinity screening, the RT–PCR product was cloned using a PCR cloning kit (Qiagen) and sequenced with an ABI PRISM 3100 Genetic Analyzer (Applied Biosystems).

Sequence analysis

The selected clones were subjected to nucleotide–nucleotide BLAST (BLASTN) search (18) to identify the protein represented by each clone. The nucleotide database obtained from the NCBI ftp site (ftp://ftp.ncbi.nlm.nih.gov/blast/db/) was employed as a reference database. The threshold of the *E*-value was configured at 1.0×10^{-1}. Clustering of the clones was performed using the CLUSTALW program (19).

Real-time PCR analysis

Real-time PCR were performed with LightCycler FastStart DNA master SYBR green I kit (Roche) and protein-specific primer sets (Supplementary Table 1) on the LightCycler (Roche). The standard template DNA was PCR-amplified from each selected sequence on pDrive vectors (Qiagen) using primers, 5′M13F (5′-GTTTTCCCAGTCACGACGTTG-3′) and 3′M13R (5′-GAAACAGCTATGACCATGATTACG-3′).

Pull-down assay

Pull-down assay using the C-terminal fluorescence labeling technique was performed according to the method of Miyamoto-Sato *et al*. (16). The DNA templates were PCR-amplified from the cloned plasmids with primers, 5′F3 and 3′R3 (5′-TTTTTTTTCTCGAGCTTGTCGTCATCG-3′). The amplicons were used as templates for transcription. The resulting mRNAs were translated in the presence of fluorescence-labeled puromycin to make fluorescence-labeled proteins. Bait Jun was also translated in the cell-free translation system separately. These translated proteins were mixed together, incubated with rabbit IgG agarose beads, and washed as described above. The binding proteins were eluted with sample buffer (0.1 M Tris–HCl, pH 6.8, 4% SDS, 0.2% bromophenol blue and 20% glycerol) at 100°C for 5 min, subjected to 17.5% SDS–PAGE, and analyzed with a Molecular Imager FX (Bio-Rad Laboratories).

Co-immunoprecipitation assay

Full-length cDNA of Jun was inserted into a pCMV-Tag5 expression vector (Stratagene). DNA fragments of the selected proteins were subcloned into the pQBI25f expression vector (Qbiogene), in which the peptide linker has been replaced with a HL4 helix linker (20) and a C-terminal FLAG-tag added. Neuro2a cells were co-transfected with both pCMV-Tag5 coding Jun and pQBI25f coding each selected protein sequence or GFP-HL4-FLAG alone (mock) using LipofectAMINE2000 (Invitrogen). After 24 h, the cells in a 6 cm dish were rinsed once with ice-cold phosphate-buffered saline (PBS) and scraped using cell-scrapers with 1.5 ml of PBS. The cells in the suspension were collected by centrifugation at 5000 r.p.m. for 5 min and lysed in 375 µl of NP lysis buffer (20 mM Tris–HCl, pH 7.6, 150 mM NaCl, 1.0% NP-40, 50 mM NaF, 1 mM Na_3VO_4 and 2 mM EDTA) containing a Complete protease inhibitor cocktail (Roche) with sonication for 1 min at 170 W and rotation for 1 h at 4°C. The lysate was centrifuged at 15 000 r.p.m. for 15 min at 4°C. An aliquot of 15 µl of the supernatant was separated and used for western-blot analysis to compare protein expression levels. For co-immunoprecipitation, 30 µl of anti-FLAG M2 agarose beads (Sigma) was added to 350 µl of the cell lysate and the mixture was incubated 2 h at 4°C with rotation. Finally, the agarose beads were washed four times with lysis buffer and resuspended in SDS–PAGE loading buffer for immunoblot analysis.

For western-blot analysis, the polyacrylamide gel was transferred onto a PVDF membrane. Duplicate blots were made from the identical immunoprecipitation experiment. One blot was probed with a rabbit anti-Jun polyclonal antibody (Calbiochem) to detect co-immunoprecipitated Jun, and the other was probed with a rabbit anti-green fluorescent protein (GFP) polyclonal antibody (Molecular Probes) to monitor the amount of GFP- and FLAG-tagged selected proteins that had been immunoprecipitated by the anti-FLAG M2 agarose beads in each reaction. The blots were revealed by an ECF western blotting kit (Amersham Biosciences) and Molecular Imager FX.

Subcellular localization analysis

COS7 cells in a 3.5 cm glass dish were co-transfected with an expression vector pQBI25f coding each newly selected protein fragment interacting with Jun *in vitro*, selected Fos, or GFP-HL4-FLAG alone (mock), together with an expression vector pCMV-Tag5B coding full-length Jun, using LipofectAMINE2000 reagent for 24 h. Before observation, the transfected cells were treated with 100 ng/ml of Hoechst33342 (Molecular Probes) for 5 min to stain the nucleus. The cells transfected with each GFP-tagged protein were observed with an Axiovert 200 M system (Carl Zeiss).

Functional clustering using annotation data

The functional annotations of the selected proteins were searched in the entries under Gene Ontology (GO) in the Mouse Genome Informatics (MGI) website (http://www.informatics.jax.org/) and those under Refseq in the Locuslink website (http://www.ncbi.nlm.nih.gov/LocusLink/). The selected proteins were clustered based on the common terms of the annotations.

RESULTS

Preparation and confirmation of IVV template library

Figure 1A shows the principle of the formation of an IVV molecule, a conjugate of protein (phenotype) and RNA (genotype). A library of IVV molecules was constructed from a cDNA library derived from mouse brain poly(A)$^+$ RNA. Because each process in the IVV template construction, i.e. reverse transcription, ligation of the PEG Puro spacer, and especially PCR-amplification (21), can be a cause of bias, which may prevent enrichment of specifically selected clones, we confirmed that no significant bias had occurred in the process of construction of the IVV template library before affinity selection. We performed RT–PCR analysis for several genes with specific primers to compare the amounts in the original mouse brain poly(A)$^+$ RNA and the constructed IVV template RNA library: all genes tested were found in both libraries in almost equal amounts (data not shown). The result indicates that this IVV template library is suitable for selection. Indeed, this test of the library was critical for success in the selection of novel interactions.

Co-translation of IVV library and bait protein

As shown in Figure 1B, we employed cell-free co-translation of bait protein with the IVV library. This protocol does not require a separate preparation of bait proteins, as was performed in the previous study (14). Thus, we considered that this convenient approach would be more suitable for high-throughput screening for protein–protein interactions. We examined the optimal concentration of mRNA template for bait Jun (Figure 1C) to generate a sufficient amount of bait protein in a cell-free translation system. The largest amount of the bait protein (~10 ng/µl) was obtained when the mRNA concentration was 200 nM (data not shown).

Selection of Jun-associated proteins from cDNA library

We then applied the IVV selection system to discover Jun-associated proteins in the mouse brain cDNA library. We performed two different kinds of selection, one being selection of the IVV library in the presence of the Jun bait protein, and the other being selection in the absence of the bait protein. Co-translated bait protein with its interactors was captured by IgG agarose beads through the added affinity tag. After five rounds of selection, the resulting libraries were cloned and sequenced. Consequently, 217 clones were obtained from the 5th round library of the bait (+) selection, and 151 clones were obtained from the 5th round library of the bait (−) selection. In the bait (−) library, it seems that materials specifically bound to the rabbit IgG agarose beads are enriched, and thus we considered clones also detected in the bait (−) library to be false positives [50 of 217 clones in the bait (+) library were removed in this step]. This simple approach to remove false positives was lacking in the previous protocols of mRNA display (14) and other display technologies (22).

Also, 24 clones including stop codons were removed, because such clones cannot form IVV and thus cannot interact with the bait protein as an IVV containing a protein moiety. The remaining 143 clones were subjected to nucleotide-nucleotide BLAST (BLASTN) search to identify the coded

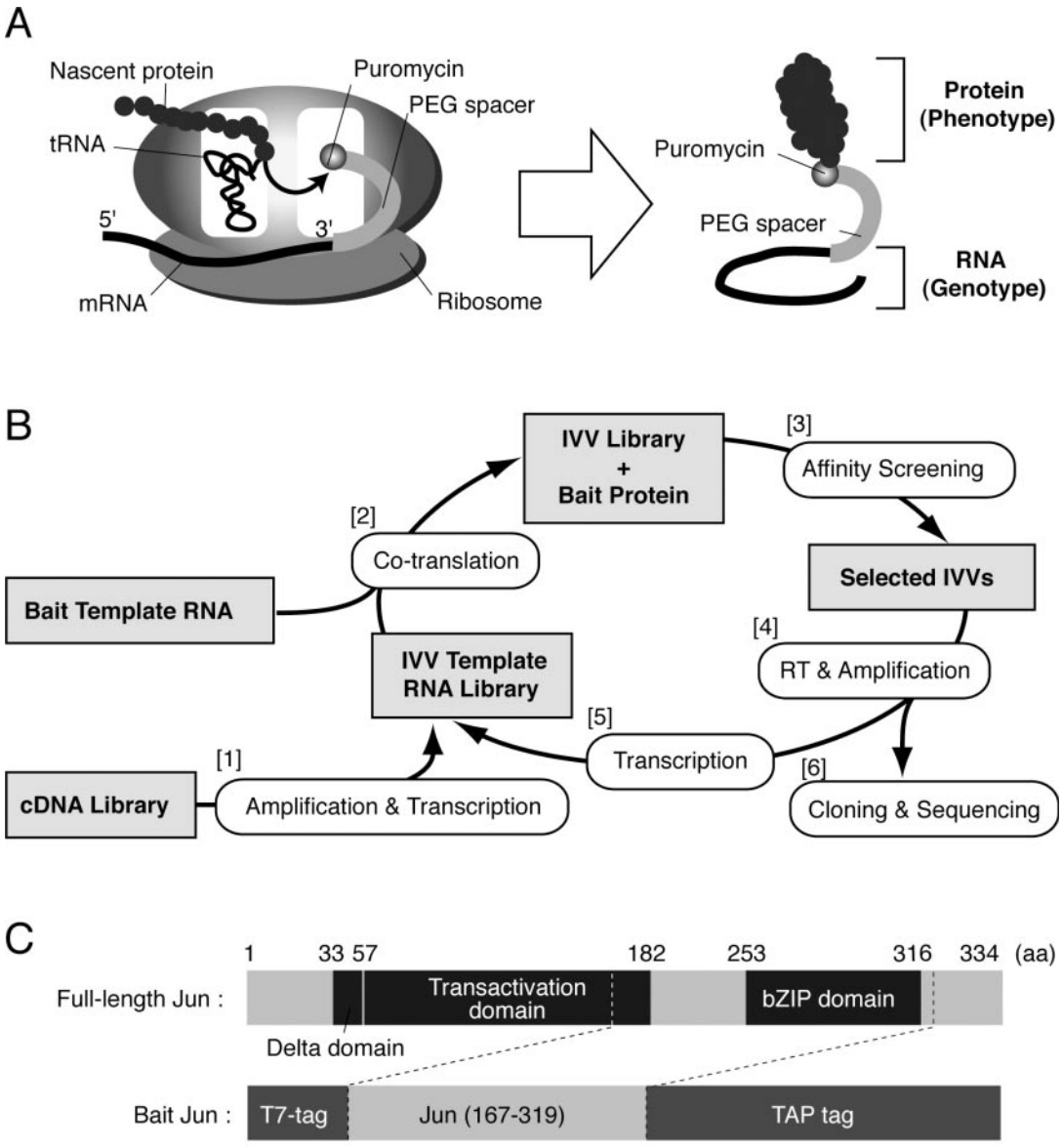

Figure 1. IVV selection of Jun-associated proteins. (**A**) Principle of IVV formation on the ribosome in a cell-free translation system (8). Puromycin ligated to the 3′-terminal end of mRNA through the polyethyleneglycol (PEG) spacer (16) can enter the ribosomal A site to bind covalently to the C-terminal end of the protein that it encodes. (**B**) Schematic representation of iterative selection for protein–protein interactions using IVV. [1] A cDNA library encoding various proteins is PCR-amplified, transcribed and ligated with a PEG spacer having puromycin. [2] The IVV template RNA library and bait template RNA are co-translated in a cell-free translation system. [3] The complex of bait protein and IVV library are subjected to affinity selection. [4] The RNA portion of the bound IVVs is reverse-transcribed and PCR-amplified. [5] The RT–PCR product is subjected to the next round of selection or [6] identified by cloning and sequencing. (**C**) Construction of the bait Jun for the selection. Jun protein has three conserved domains, delta domain, transactivation domain and bZIP domain. As a bait, the fragment containing the bZIP domain of Jun was fused with a T7-tag for confirmation of expression of the bait protein and with the TAP affinity selection tag, which contains the IgG binding domain of protein A, TEV protease cleavage site and calmodulin binding peptide (1).

proteins. Of the 143 clones, 7 were further removed, because these clones corresponded to 5′-untranslated region (5′-UTR) or 3′-UTR in mRNA sequences. Consequently, a total of 81 clones (37% of total clones) were eliminated from the obtained 217 clones as false positives. Surviving clones from the above examinations were further characterized.

The remaining 136 clones were clustered into 20 distinct sequence groups by the CLUSTALW algorithm (Table 1). Ten of the clusters consist of siblings, and the others consist of single clones (Table 1). BLASTN search revealed that 16 of the clusters involved known proteins. The other four proteins, 4732436F15Rik, 9130229H14Rik, 1200008A14Rik and B130050I23Rik, are hypothetical proteins, which have been reported in the full-length cDNA sequencing and functional annotation project ‘FANTOM2’ (23). Characterization of the amino acid sequences revealed that 14 of the 20 proteins contain leucine heptad repeats, which have the potential to form a leucine zipper motif. Four of the 20 proteins, Fos, Jun, Atf4 and Jdp2, have already been reported to interact with Jun directly (24), but the other 16 have not. Thus, we further examined their specific interactions with Jun by means of real-time PCR, *in vitro* pull-down assays and co-immunoprecipitation assays.

Table 1. A total of 20 selected proteins from IVV selection and sequence analyses

Gene symbol	Accession no.	Number of clones	Locus on mRNA sequence (base)	Previous report	Leucine heptad repeats	*In vitro* pull-down assay[a]
SNAP19	NM_183316.1	78	1...285	Unknown	Y	++
Kif5C (region C)	NM_008449.1	17	2473...2672	Unknown	Y	+
Kif5A (region C)	NM_008447.2	5	2654...2851	Unknown	Y	+
Eef1d	NM_023240.1	5	149...522	Unknown	Y	ND[b]
Jdp2	NM_030887.2	5	481...717	Known	Y	+++
Kif5C (region N)	NM_008449.1	4	907...1115	Unknown	N	—
Nef3	NM_008691.1	4	1086...1251	Unknown	N	—
4732436F15Rik	XM_143418.3	3	2087...2287	Unknown	Y	++
Fos	NM_010234.2	3	493...740	Known	Y	+++
9130229H14Rik	XM_135706.3	2	96...267	Unknown	Y	++
Atf4	NM_009716.1	1	1091...1305	Known	Y	+
Mapre3	NM_133350.1	1	724...980	Unknown	N	+
Cspg6	NM_007790.2	1	2474...2689	Unknown	Y	++
Mapk8ip3	NM_013931.1	1	1413...1624	Unknown	Y	+
Jun	NM_010591.1	1	904...1036	Known	Y	++
1200008A14Rik	NM_028915.1	1	1522...1677	Unknown	Y	+
GFAP	K01347.1	1	892...1025	Unknown	N	—
B130050I23Rik	NM_153536.2	1	1151...1424	Unknown	Y	++
Kif5A (region N)	NM_008447.2	1	1427...1463	Unknown	N	—
Kif5B (region N)	NM_008448.1	1	1229...1362	Unknown	N	—

[a]Interaction level of selected proteins with bait Jun based on the result of pull-down assay: —, none; +, weak; ++, strong; +++, very strong; and ND, no data.
[b]Eef1d contains leucine heptad repeats, and significant interaction was observed in the presence of bait protein, but similar behavior was also observed in the absence of bait protein.

Quantitative analysis of selected protein clones using real-time PCR

The finally selected clones may merely contain RNA that is abundant in the initial library, such as β-actin. Such negative clones can be distinguished from positive clones that are expected to be enriched in the bait (+) selection, but not enriched in the bait (−) selection. Thus, we used real-time PCR analysis to determine the amounts of the DNA molecules encoding the selected proteins in the DNA libraries from each round of the selection. Of the 20 candidates, 19 selected proteins were enriched in each round in the presence of Jun bait. The enrichment rates were between 80- and 2.0×10^4-fold, while β-actin (negative control) was not enriched. In contrast, none of the selected proteins, nor β-actin, was enriched in the bait (−) selection. These results support the conclusion that the 19 selected proteins were specifically enriched by interacting directly or indirectly with Jun bait protein. In the initial library and in the 5th bait (+), library the 19 proteins accounted for less than 0.1% and over 50% of the total, respectively. The region N of Kif5A with a chain length of 38 bp was not analyzed, because the clone was too short to perform real-time PCR analysis.

Verification of protein–protein interactions *in vitro* by pull-down assay

To determine whether the selected proteins have the ability to interact directly with Jun, *in vitro* pull-down assay was performed. A C-terminal-specific fluorescence labeling technique, which is a simple and convenient method (25), was employed for the pull-down assay. As shown in Table 1, 14 proteins including 4 known positives, Jun, Fos, Atf4 and Jdp2, exhibited direct interactions with Jun bait protein *in vitro*. All of the 14 proteins, except for Mapre3, contain leucine heptad repeats. The other proteins, Kif5A (region N), Kif5B (region N), Kif5C (region N), Nef3 and GFAP, except for Eef1d (see Table 1) neither interacted nor contained leucine heptad repeats. We considered that these proteins might interact with Jun indirectly via other Jun-associated proteins, because there are some findings indicating interactions between selected proteins. For example, regions C and N of Kif5 family (Kif5s) proteins (Table 1) are known to interact in a single molecule, generating a compact structure to control the motor activity of the Kif5s (26–28). The region C clones have leucine heptad repeats and interacted directly with Jun *in vitro*; thus, region N fragments of Kif5s might interact with bait Jun via region C fragments of Kif5s in this selection. Also, Nef3 are known to interact with Kif5A (29), and selected regions of Nef3 are highly homologous to parts of GFAP. Consequently, all five proteins for which direct interactions with Jun were not confirmed by pull-down assay, in spite of the specific enrichment confirmed by real-time PCR, may interact indirectly with Jun through other positive clones.

Verification of protein–protein interactions in cultured cells

Transfected Jun protein was assayed by co-immunoprecipitation with 10 GFP- and FLAG-tagged selected proteins which exhibited interaction with Jun *in vitro* (Figure 2). All 10 selected proteins were immunoprecipitated (Figure 2B, upper panels), while Jun was co-immunoprecipitated with only 6 of the 10 proteins, SNAP19, Cspg6, 9130229H14Rik, 1200008A14Rik, B130050I23Rik and 4732436F15Rik (Figure 2B, lower panels). The other four proteins, Kif5A (region C), Kif5C (region C), Mapk8ip3 and Mapre3, apparently did not interact with Jun.

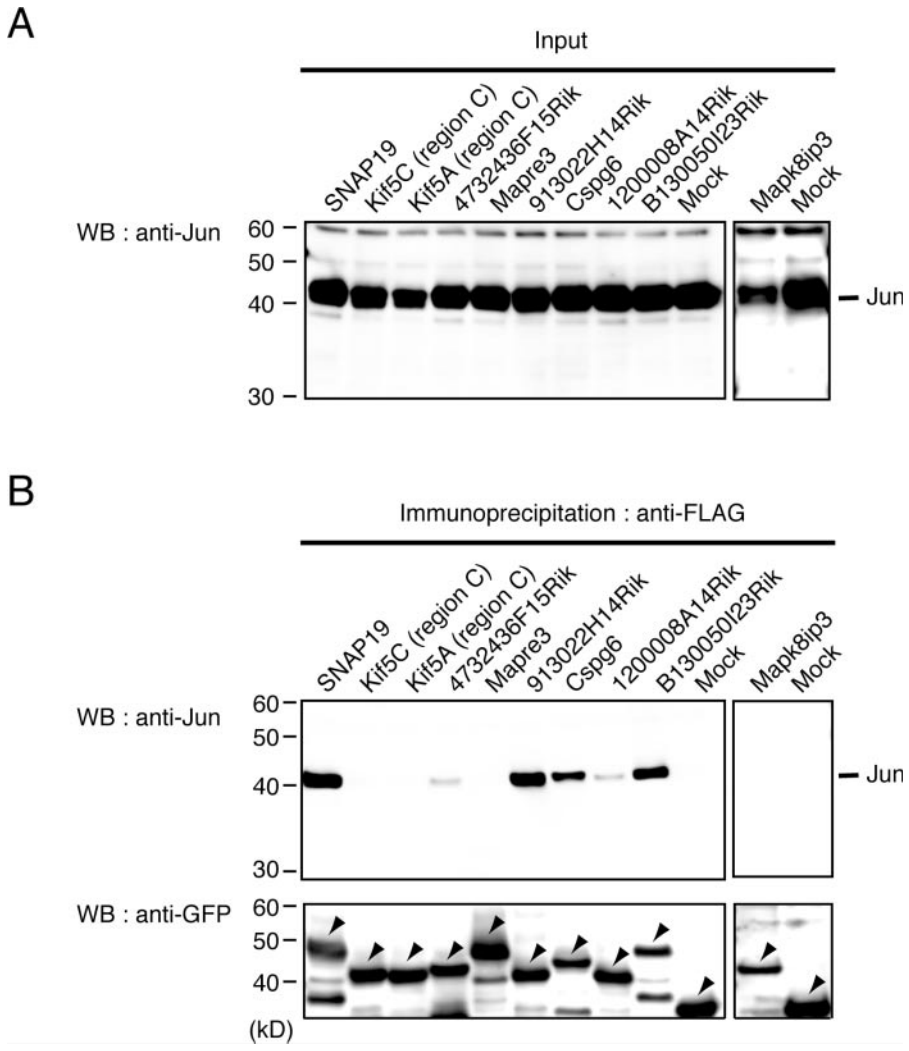

Figure 2. Co-immunoprecipitation assay between Jun and selected Jun-associated protein candidates. (**A**) Western-blot analysis, showing the expression levels of Jun after co-transfection with Jun and each of 10 selected proteins. 'Mock' was co-transfected with Jun and GFP-HL4-FLAG. (**B**) Extracts of COS7 cells which were transfected with Jun and each of the ten selected proteins were immunoprecipitated with anti-FLAG antibody. This was followed by western-blot analysis using the anti-Jun antibody to detect co-immunoprecipitated Jun protein (top) and anti-GFP antibody to detect GFP-fused selected proteins (arrowhead on the bottom).

Determination of subcellular localization of selected protein fragments

To elucidate why the interaction of some proteins that interacted with Jun *in vitro* could not be confirmed by co-immunoprecipitation assay, we observed the subcellular localization of 10 GFP-tagged selected protein fragments in COS7 cells (Figure 3). As a control, a GFP-tagged selected Fos protein fragment and GFP-HL4-FLAG protein alone (mock) were also transfected. All of the protein fragments that were co-immunoprecipitated with Jun, SNAP19, 4732436F15Rik, 913022H14Rik, Cspg6 and B130050I23Rik, except for 1200008A14Rik, were located mostly in the nucleus, like Fos. On the other hand, the proteins that did not co-immunoprecipitate Jun, Kif5C (region C), Kif5A (region C), Mapre3 and Mapk8ip3, were located mostly in cytoplasm. Mock protein was located ubiquitously in the cells. These results imply that differences in the subcellular localization of the transfected protein fragments could explain the result of the co-immunoprecipitation assay.

Prediction of cellular function

In order to elucidate the cellular roles of the selected proteins, functional annotations of these proteins in public databases were searched from the entries in GO and Refseq. As shown in Figure 4, the 13 unreported proteins and 4 known positives were clustered into five functional groups, microtubule association (Kif5A, Kif5B, Kif5C and Mapre3), kinesin complex (GFAP, Nef3, Kif5A, Kif5B, Kif5C, Mapk8ip3 and Cspg6), chromosome segregation (Cspg6, 9130229H14Rik and 1200008A14Rik), DNA repair (Mapk8ip3, Cspg6 and 9130229H14Rik), and transcriptional regulation (SNAP19, Fos, Jdp2, Atf4 and Jun). Two hypothetical proteins, B130050I23Rik and 4732436F15Rik, have no clear functional annotations (black-bordered boxes in Figure 4).

DISCUSSION

Jun protein is a eukaryotic transcription factor, which plays an important role in a variety of cellular functions, including

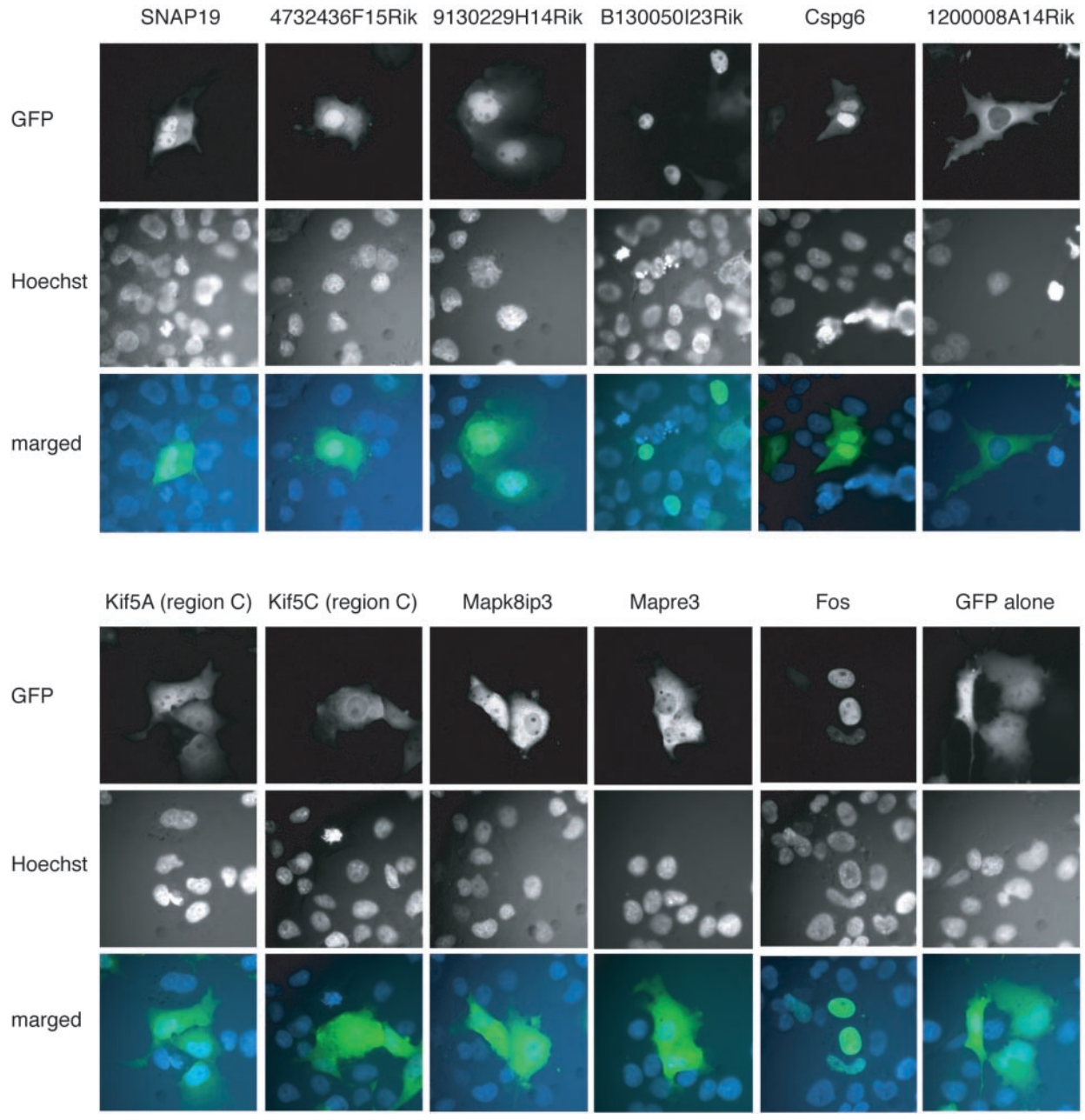

Figure 3. Subcellular localization of the 10 selected protein fragments. COS7 cells were transfected with GFP-tagged selected protein fragments that interacted with Jun *in vitro*, GFP-tagged selected Fos fragment, and GFP-HL4-FLAG alone (negative control). The Fos fragment was used as a positive control of co-localization with Jun, because it was efficiently co-immunoprecipitated with Jun. Upper panels show GFP-tagged proteins. Middle panels show the nucleus stained with Hoechst33342. Lower panels show merged images. GFP and Hoechst33342 appear as green and blue, respectively.

proliferation, differentiation and tumorigenesis (30). The cellular functions of Jun vary according to the interacting partners (24). So far, over 50 Jun-associated proteins have been found in various tissues by using biochemical methods, Y2H assay, and other techniques (24). Jun forms a homodimer and heterodimers with Fos/Jun family proteins such as Fos, Fra1, Fra2, FosB, Jun, JunB and JunD (31–34), and with other bZIP family proteins (24). Jun also interacts directly with many proteins, such as transcriptional co-activators, structurally unrelated DNA binding proteins and nuclear structural components (24). Most of the known Jun-associated proteins are transcriptional regulators.

In this study, we were able to select 20 candidate Jun-associated proteins from a mouse brain cDNA library by using the IVV selection system. Of the 20 candidates, 16 are previously unreported interactions. Of the 16 selected proteins, 10 proteins were confirmed to interact directly with Jun bait protein *in vitro* (Table 1). All 10 proteins, except for Mapre3, contain leucine heptad repeats. This result seems reasonable, because almost all Jun-associated proteins that interact with the bZIP domain of Jun have a leucine zipper motif, which is essential to form heterodimers with Jun (24). Furthermore, 6 of the 10 candidates, SNAP19, Cspg6, 9130229H14Rik, 1200008A14Rik, B130050I23Rik and

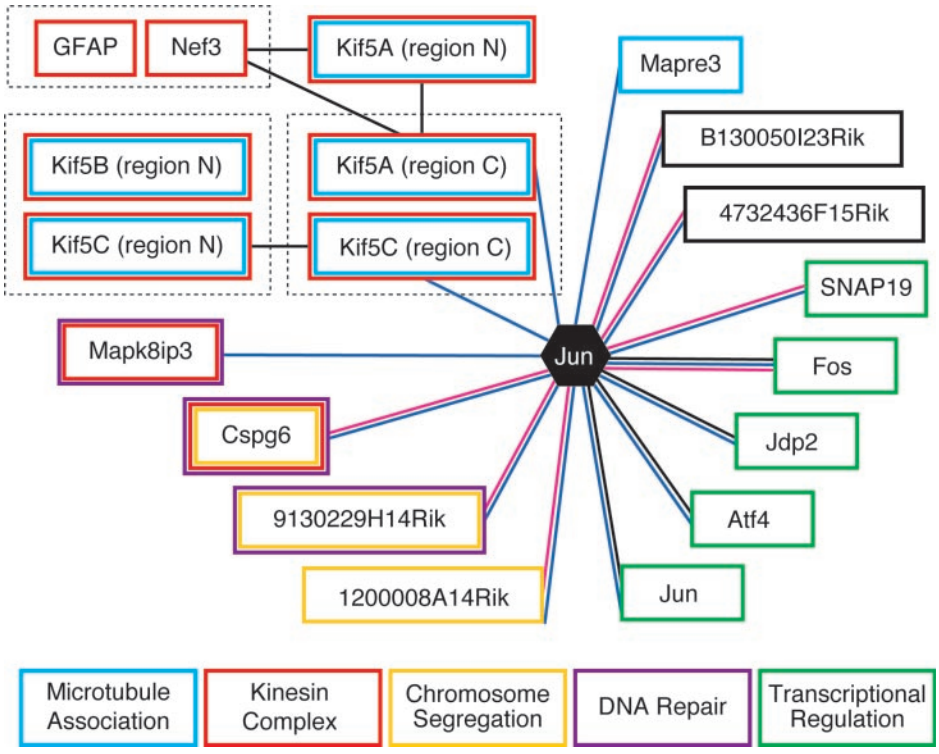

Figure 4. Protein–protein interaction mapping of the selected proteins with functional annotations. Protein–protein interactions confirmed by co-immunoprecipitation and pull-down assay are represented as magenta and blue lines, respectively. Black lines indicate previously reported interactions. Color-bordered boxes represent the functional annotations of the proteins as indicated in the lower panels. Two hypothetical proteins (black-bordered boxes) have no clear functional annotations. Broken-lined squares represent highly homologous protein fragment pairs.

4732436F15Rik, were confirmed to interact with Jun in a cultured cell line by using co-immunoprecipitation assay (Figure 2). We predicted the cellular functions of these proteins by means of functional clustering using annotations.

SNAP19, the most abundant protein (Table 1; 57% of the positives) in this selection, was clustered into the functional group of transcriptional regulation (Figure 4). SNAP19 is known as a 19 kDa subunit of a small nuclear RNA-activating protein complex (35). Previous reports indicate that SNAP19 works in the nucleus as a subunit of the transcriptional regulator protein complex (35). Although no functional or physical relationship between SNAP19 and Jun has been reported previously, our present findings strongly suggest an interaction between SNAP19 and Jun in living cells.

Cspg6, 9130229H14Rik and 1200008A14Rik were clustered into two functional groups, DNA repair and chromosome segregation. This suggests that Jun plays unreported roles in these functions (Figure 4). There are some examples of transcription factors with other non-transcriptional cellular functions; for example, a bZIP transcription factor controls the cell cycle by interacting directly with Cdk2 protein without the involvement of any transcriptional event (36), and an unexpected interaction of Jun with cytoskeletal materials has been reported recently (37). Otherwise our selected proteins may work cooperatively with Jun as transcriptional regulators. For example, Mmip1 protein, an isoform of Cspg6, was reported as a transcriptional suppressor interacting with Mad proteins, a bHLH-ZIP transcriptional regulator family (38,39), implying that Cspg6 protein may also suppress the transcriptional activity of Jun.

Although B130050I23Rik and 4732436F15Rik have no clear annotation, their nuclear localization predicted by the PSORTII program (http://psort.nibb.ac.jp) implies interaction with Jun in the nucleus *in vivo*, and possible functions related to transcriptional regulation. Further *in vivo* experiments are necessary to clarify these proteins' cellular functions.

We could not confirm the interactions between Jun and the other four candidates, Kif5A (region C), Kif5C (region C), Mapk8ip3 and Mapre3, by means of co-immunoprecipitation assay (Figure 2), in spite of the *in vitro* interactions. A possible reason for this would be a difference of subcellular localization between these proteins and Jun. Indeed, all of the proteins that were confirmed to interact with Jun in cultured cells, except for 1200008A14Rik, were located mostly in the nucleus, like Fos protein, a well-known Jun-interactor, while the above-mentioned four proteins were located mostly in cytoplasm (Figure 3), and are known to interact with the cytoskeleton in living cells (40–42). Although the *in vitro* interactions of these four proteins may be biological false positives, biologically significant interaction with Jun cannot be ruled out, because subcellular localizations of some proteins are known to be tightly restricted to a specific phase *in vivo*. For example, Kif17, a closely related paralogous protein of Kif5 family proteins, is located in the nucleus and interacts with ACT protein, a transcriptional co-activator, only at the specific stage of spermatogenesis *in vivo*, and the interaction was only confirmed by immunostaining analysis of mouse testis tissue (43).

So far, genome-wide analyses of protein–protein interactions have been performed by only Y2H and biochemical

methods using MS. The IVV selection system exemplified in this study has several advantages over previous techniques, for example, convenient removability of false positives arising from the selection system itself, availability of a wider range of interacting conditions and availability for analysis of the interactions of toxic proteins. Every current technique for screening of protein–protein interactions has some disadvantages as well as advantages, and therefore the use of a range of different techniques is important to obtain as complete a map as possible of protein–protein interactions in various organisms.

SUPPLEMENTARY MATERIAL

Supplementary Material is available at NAR Online.

ACKNOWLEDGEMENTS

We thank Dr Takashi Takeuchi for experimental advice. This work was supported in part by a Grant-in-Aid for the 21st Century Center of Excellence (COE) Program entitled 'Understanding and Control of Life's Function via Systems Biology (Keio University)' and a Special Coordination Fund of the Ministry of Education, Culture, Sports, Science and Technology, Japan.

REFERENCES

1. Puig,O., Caspary,F., Rigaut,G., Rutz,B., Bouveret,E., Bragado-Nilsson,E., Wilm,M. and Seraphin,B. (2001) The tandem affinity purification (TAP) method: a general procedure of protein complex purification. *Methods*, **24**, 218–229.
2. Fields,S. and Song,O. (1989) A novel genetic system to detect protein–protein interactions. *Nature*, **340**, 245–246.
3. Vidalain,P.O., Boxem,M., Ge,H., Li,S. and Vidal,M. (2004) Increasing specificity in high-throughput yeast two-hybrid experiments. *Methods*, **32**, 363–370.
4. Smith,G.P. (1985) Filamentous fusion phage: novel expression vectors that display cloned antigens on the virion surface. *Science*, **228**, 1315–1317.
5. Bradbury,A.R. and Marks,J.D. (2004) Antibodies from phage antibody libraries. *J. Immunol. Methods*, **290**, 29–49.
6. Hanes,J. and Pluckthun,A. (1997) *In vitro* selection and evolution of functional proteins by using ribosome display. *Proc. Natl Acad. Sci. USA*, **94**, 4937–4942.
7. Mattheakis,L.C., Bhatt,R.R. and Dower,W.J. (1994) An *in vitro* polysome display system for identifying ligands from very large peptide libraries. *Proc. Natl Acad. Sci. USA*, **91**, 9022–9026.
8. Nemoto,N., Miyamoto-Sato,E., Husimi,Y. and Yanagawa,H. (1997) *In vitro* virus: bonding of mRNA bearing puromycin at the 3′-terminal end to the C-terminal end of its encoded protein on the ribosome *in vitro*. *FEBS Lett.*, **414**, 405–408.
9. Miyamoto-Sato,E., Nemoto,N., Kobayashi,K. and Yanagawa,H. (2000) Specific bonding of puromycin to full-length protein at the C-terminus. *Nucleic Acids Res.*, **28**, 1176–1182.
10. Roberts,R.W. and Szostak,J.W. (1997) RNA–peptide fusions for the *in vitro* selection of peptides and proteins. *Proc. Natl Acad. Sci. USA*, **94**, 12297–12302.
11. Yonezawa,M., Doi,N., Kawahashi,Y., Higashinakagawa,T. and Yanagawa,H. (2003) DNA display for *in vitro* selection of diverse peptide libraries. *Nucleic Acids Res.*, **31**, e118.
12. Takahashi,T.T., Austin,R.J. and Roberts,R.W. (2003) mRNA display: ligand discovery, interaction analysis and beyond. *Trends Biochem. Sci.*, **28**, 159–165.
13. Lipovsek,D. and Pluckthun,A. (2004) *In-vitro* protein evolution by ribosome display and mRNA display. *J. Immunol. Methods*, **290**, 51–67.
14. Hammond,P.W., Alpin,J., Rise,C.E., Wright,M. and Kreider,B.L. (2001) *In vitro* selection and characterization of Bcl-X(L)-binding proteins from a mix of tissue-specific mRNA display libraries. *J. Biol. Chem.*, **276**, 20898–20906.
15. Cujec,T.P., Medeiros,P.F., Hammond,P., Rise,C. and Kreider,B.L. (2002) Selection of v-abl tyrosine kinase substrate sequences from randomized peptide and cellular proteomic libraries using mRNA display. *Chem. Biol.*, **9**, 253–264.
16. Miyamoto-Sato,E., Takashima,H., Fuse,S., Sue,K., Ishizaka,M., Tateyama,S., Horisawa,K., Sawasaki,T., Endo,Y. and Yanagawa,H. (2003) Highly stable and efficient mRNA templates for mRNA–protein fusions and C-terminally labeled proteins. *Nucleic Acids Res.*, **31**, e78.
17. Sawasaki,T., Ogasawara,T., Morishita,R. and Endo,Y. (2002) A cell-free protein synthesis system for high-throughput proteomics. *Proc. Natl Acad. Sci. USA*, **99**, 14652–14657.
18. Altschul,S.F., Gish,W., Miller,W., Myers,E.W. and Lipman,D.J. (1990) Basic local alignment search tool. *J. Mol. Biol.*, **215**, 403–410.
19. Thompson,J.D., Higgins,D.G. and Gibson,T.J. (1994) CLUSTAL W: improving the sensitivity of progressive multiple sequence alignment through sequence weighting, position-specific gap penalties and weight matrix choice. *Nucleic Acids Res.*, **22**, 4673–4680.
20. Arai,R., Ueda,H., Kitayama,A., Kamiya,N. and Nagamune,T. (2001) Design of the linkers which effectively separate domains of a bifunctional fusion protein. *Protein Eng.*, **14**, 529–532.
21. Kanagawa,T. (2003) Bias and artifacts in multitemplate polymerase chain reactions (PCR). *J. Biosci. Bioeng.*, **96**, 317–323.
22. Hertveldt,K., Dechassa,M.L., Robben,J. and Volckaert,G. (2003) Identification of Gal80p-interacting proteins by *Saccharomyces cerevisiae* whole genome phage display. *Gene*, **307**, 141–149.
23. Okazaki,Y., Furuno,M., Kasukawa,T., Adachi,J., Bono,H., Kondo,S., Nikaido,I., Osato,N., Saito,R., Suzuki,H. *et al.* (2002) Analysis of the mouse transcriptome based on functional annotation of 60,770 full-length cDNAs. *Nature*, **420**, 563–573.
24. Chinenov,Y. and Kerppola,T.K. (2001) Close encounters of many kinds: Fos–Jun interactions that mediate transcription regulatory specificity. *Oncogene*, **20**, 2438–2452.
25. Doi,N., Takashima,H., Kinjo,M., Sakata,K., Kawahashi,Y., Oishi,Y., Oyama,R., Miyamoto-Sato,E., Sawasaki,T., Endo,Y. *et al.* (2002) Novel fluorescence labeling and high-throughput assay technologies for *in vitro* analysis of protein interactions. *Genome Res.*, **12**, 487–492.
26. Stock,M.F., Guerrero,J., Cobb,B., Eggers,C.T., Huang,T.G., Li,X. and Hackney,D.D. (1999) Formation of the compact confomer of kinesin requires a COOH-terminal heavy chain domain and inhibits microtubule-stimulated ATPase activity. *J. Biol. Chem.*, **274**, 14617–14623.
27. Friedman,D.S. and Vale,R.D. (1999) Single-molecule analysis of kinesin motility reveals regulation by the cargo-binding tail domain. *Nature Cell Biol.*, **1**, 293–297.
28. Seiler,S., Kirchner,J., Horn,C., Kallipolitou,A., Woehlke,G. and Schliwa,M. (2000) Cargo binding and regulatory sites in the tail of fungal conventional kinesin. *Nature Cell Biol.*, **2**, 333–338.
29. Xia,C.H., Roberts,E.A., Her,L.S., Liu,X., Williams,D.S., Cleveland,D.W. and Goldstein,L.S. (2003) Abnormal neurofilament transport caused by targeted disruption of neuronal kinesin heavy chain KIF5A. *J. Cell Biol.*, **161**, 55–66.
30. Shaulian,E. and Karin,M. (2002) AP-1 as a regulator of cell life and death. *Nature Cell Biol.*, **4**, E131–136.
31. Kovary,K. and Bravo,R. (1991) Expression of different Jun and Fos proteins during the G_0-to-G_1 transition in mouse fibroblasts: *in vitro* and *in vivo* associations. *Mol. Cell. Biol.*, **11**, 2451–2459.
32. Lallemand,D., Spyrou,G., Yaniv,M. and Pfarr,C.M. (1997) Variations in Jun and Fos protein expression and AP-1 activity in cycling, resting and stimulated fibroblasts. *Oncogene*, **14**, 819–830.
33. McCabe,L.R., Kockx,M., Lian,J., Stein,J. and Stein,G. (1995) Selective expression of fos- and jun-related genes during osteoblast proliferation and differentiation. *Exp. Cell Res.*, **218**, 255–262.
34. Sonnenberg,J.L., Macgregor-Leon,P.F., Curran,T. and Morgan,J.I. (1989) Dynamic alterations occur in the levels and composition of transcription factor AP-1 complexes after seizure. *Neuron*, **3**, 359–365.
35. Henry,R.W., Mittal,V., Ma,B., Kobayashi,R. and Hernandez,N. (1998) SNAP19 mediates the assembly of a functional core promoter complex (SNAPc) shared by RNA polymerases II and III. *Genes Dev.*, **12**, 2664–2672.
36. Izumiya,Y., Lin,S.F., Ellison,T.J., Levy,A.M., Mayeur,G.L., Izumiya,C. and Kung,H.J. (2003) Cell cycle regulation by Kaposi's

sarcoma-associated herpesvirus K-bZIP: direct interaction with cyclin-CDK2 and induction of G1 growth arrest. *J. Virol.*, **77**, 9652–9661.
37. Luettich,K. and Schmidt,C. (2003) TGFbeta1 activates c-Jun and Erk1 via alphaVbeta6 integrin. *Mol. Cancer*, **2**, 33.
38. Gupta,K., Anand,G., Yin,X., Grove,L. and Prochownik,E.V. (1998) Mmip1: a novel leucine zipper protein that reverses the suppressive effects of Mad family members on c-myc. *Oncogene*, **16**, 1149–1159.
39. Jones,S. and Sgouros,J. (2001) The cohesin complex: sequence homologies, interaction networks and shared motifs. *Genome Biol.*, **2**, RESEARCH0009.
40. Kanai,Y., Okada,Y., Tanaka,Y., Harada,A., Terada,S. and Hirokawa,N. (2000) KIF5C, a novel neuronal kinesin enriched in motor neurons. *J. Neurosci.*, **20**, 6374–6384.
41. Verhey,K.J., Meyer,D., Deehan,R., Blenis,J., Schnapp,B.J., Rapoport,T.A. and Margolis,B. (2001) Cargo of kinesin identified as JIP scaffolding proteins and associated signaling molecules. *J. Cell Biol.*, **152**, 959–970.
42. Nakagawa,H., Koyama,K., Murata,Y., Morito,M., Akiyama,T. and Nakamura,Y. (2000) EB3, a novel member of the EB1 family preferentially expressed in the central nervous system, binds to a CNS-specific APC homologue. *Oncogene*, **19**, 210–216.
43. Macho,B., Brancorsini,S., Fimia,G.M., Setou,M., Hirokawa,N. and Sassone-Corsi,P. (2002) CREM-dependent transcription in male germ cells controlled by a kinesin. *Science*, **298**, 2388–2390.